Analysis of Curved Target-Type Thrust Reversers

Turgut Sarpkaya

Naval Postgraduate School, Monterey, Calif.

And

Gerardo Hiriart

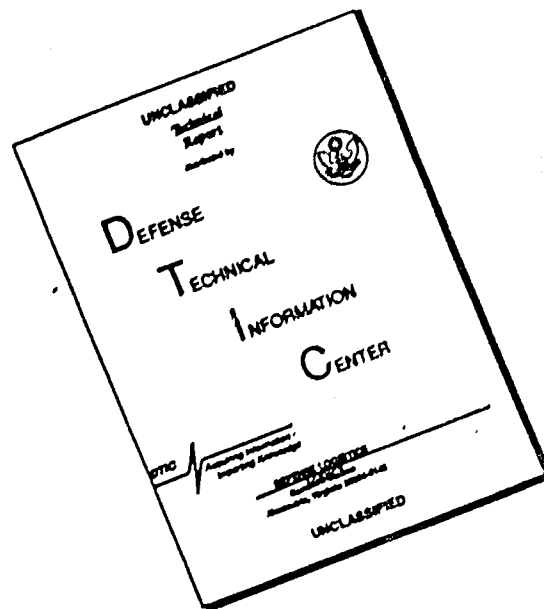*Chilean Navy, Santiago, Chile*

D D

JUL 3 1975

B

DISCLAIMER NOTICE

THIS DOCUMENT IS BEST QUALITY AVAILABLE. THE COPY FURNISHED TO DTIC CONTAINED A SIGNIFICANT NUMBER OF PAGES WHICH DO NOT REPRODUCE LEGIBLY.

Analysis of Curved Target-Type Thrust Reversers

Turgut Sarpkaya*
Naval Postgraduate School, Monterey, Calif.

AND

Gerardo Hiriart†
Chilean Navy, Santiago, Chile

The reverse-thrust performance of two-dimensional and axisymmetric curved deflectors, symmetrically situated with respect to the impinging jet, is analyzed through the use of Levi-Civita's method, Belotserkovsky's integral method, and the finite element method. The predicted results are shown to be in reasonable agreement with the available experimental data. The real-fluid effects such as Coanda effect, entrainment, and the pressure ratio are discussed in the light of the present inviscid flow analyses.

Nomenclature

a_n	= coefficients
A_i	= areas of subtriangles in a triangle
A^m	= area of a triangle
d	= jet width or diameter
$g(r)$	= reverser geometry
h	= length of the normal, Fig. 6
$h(\sigma)$	= a function
i	$= (-1)^{1/2}$
$I(\phi)$	= functional of ϕ
k	= a parameter
n	= normal axis
p	= pressure
q	= magnitude of total velocity
r	= radial distance
r_o	= nozzle radius
R	= radius of curvature
R_o	= reverser radius
s	= axis along the free surface
s_o	= nozzle setback distance
SA_{ij}^m	= element matrix for element m
SLA_i^m	= load matrix for element m
t	= a parameter, Fig. 1
u, v	= velocity components
V_j	= free streamline velocity
V_o	= normalized uniform velocity in the nozzle
W	= complex potential
x, y, z	= coordinate axes
β	= deflection angle
δ	= slope of the reverser boundary, Fig. 6b
ζ	= a variable
ζ_i	= area coordinates
η_R	= reverse-thrust ratio
θ	= direction of velocity vector
λ	= a multiplier
ρ	= density of fluid
σ	= a variable, Fig. 2
ϕ	= potential function
ψ	= stream function
ω	= a complex function

Introduction

THE fluid dynamics of a free air or liquid jet impinging on a rigid or deformable surface poses problems of special interest in the analysis of impulse machinery, thrust reversers, flip buckets on spillways, rock and metal cutting with high-

speed water jets, false-twisting of yarns, etc. A complete discussion of the mechanics of the flow situation would include the compressibility and gravitational effects, boundary-layer effects at the solid surface, and the entrainment effects at the free surface, but in most cases these are relatively unimportant, and it is sufficiently realistic to assume the fluid to be inviscid and incompressible. Even with this simplification, the prediction of the characteristics of the deflected jet may still pose exceedingly complex problems particularly for jets impinging obliquely upon prescribed boundaries. For example, the oblique impact of a round jet on a plane surface has not yet been analyzed.[1] Thus, the analysis is often restricted to two-dimensional or axisymmetric situations and recourse is usually made to approximate methods of analysis where a free surface is assumed and its suitability is assessed from approximate potential solutions obtained through the use of various numerical techniques.

The two-dimensional counterpart of the jet-deflection problem has been treated through the use of the powerful analytic-function theory and successive conformal transformations. Sarpkaya[2] solved the U-shaped, two-segment, deflector problem where the turning angle between the segments is limited to 90°. Tinney et al.[3] extended this analysis to the case where the turning angle between the symmetrically situated segments is greater than 90°. Later, Chang and Conly[4] presented an analysis for a bucket composed of a series of segments of arbitrary number, lengths, and angles. However, the basic as well as practical problem of the direct and exact analysis of jet deflection by curved buckets remained unsolved.

The three-dimensional counterpart of the jet-deflection problem has not been solved in any generality. Attempts to formulate an exact solution have been mostly unsuccessful even for axisymmetric inviscid flows with no body forces. The case of a circular jet striking a plate normally was analyzed by Schach[5] using approximate methods similar to those of Trefftz[6] with successive adjustment of the free streamlines. Jeppson[7] applied the finite difference technique to the solution of two, axisymmetric, potential-flow problems, namely to that of flow from a nozzle and the cavitating flow of a jet past a body of revolution. Other noteworthy contributions to the analysis of the jet efflux from nozzles and orifices were made by Southwell and Vaisey,[8] Rouse and Abul-Fetouh,[9] Garabedian,[10] and Hunt[11] through the use of the relaxation and finite-difference methods. Schnurr et al.[12] used the relaxation method to analyze the turning of two-dimensional and axisymmetric jets from curved surfaces where the jet was assumed to leave the deflector exactly parallel to the tangent at the lip of the deflector surface. The consequence of the difference between the actual deflection angle and the said tangent to the deflector
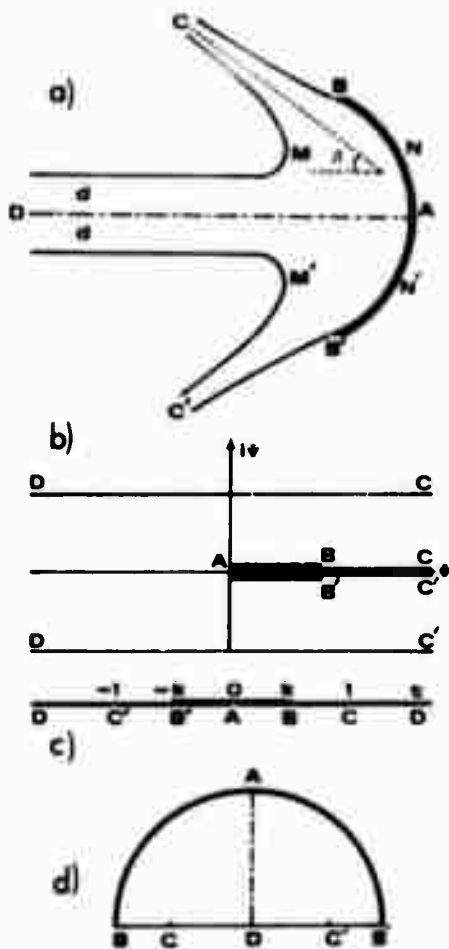
Fig. 1 Transformation planes; a) physical plane, b) W-plane, c) t-plane, and d) ζ-plane.

mentally. Thus, their analysis does not constitute a solution to the thrust-reverser problem.

Ryhming[13] studied the problem of a steady liquid jet impacting on a plane and on an infinite axisymmetric cavity by employing Belotserkovsky's[14] integral method. As in the case of Schnurr et al., the results of this work do not apply to the thrust-reverser problem where there are two free surfaces and where the asymptotic slope of the deflected jet is not parallel to the tangent at the lip of the deflector surface.

In the present work three methods are employed to investigate the deflection of inviscid, incompressible curved surfaces: Levi-Civita's method, Belotserkovsky's integral method, and the finite element method. The first method is applied to plane jets impinging symmetrically on two-dimensional curved surfaces whose shapes are specified in terms of a given jet-deflection angle and the angle of departure at the lip of the two-dimensional bucket. The other two methods are applied to straight circular jets impinging on axisymmetric curved surfaces.

Plane Jets and Two-Dimensional Curved Deflectors

The past as well as the present analyses have emphatically demonstrated that almost all of the difficulties of the analysis of jet deflection from curved obstacles are ascribable to the determination of the initially unknown free streamlines. In view of this fact a direct analysis of the problem, that is, the determination of the jet deflection angle and the position of the free streamlines via either purely analytical or partly analytical and partly numerical techniques is at best a difficult problem. As propounded by Birkhoff and Zarantonello,[15] what one can hope for is an indirect solution of the problem, i.e. obtaining a family of obstacle shapes which will yield the prescribed jet-deflection angle and provide a familiarity between the shapes so obtained and the range and change of direction of the free

parameters involved in the analysis. This holds true for both the plane and axisymmetric flows. Should one adopt a purely numerical procedure (e.g. finite difference, relaxation, finite element, marker-and-cell technique), it is then and only then possible to begin with a prescribed obstacle shape and to approach a unique solution through successive iterations.

It is well known from the free-streamline theory that whenever the solid boundaries are composed of straight segments, then the Ω-plane also is composed of straight lines (see, e.g., Ref. 16). Since such a polygonal boundary can always be transformed onto a t-plane through the use of Schwarz-Christoffel transformation, all two-dimensional jet-deflection problems of this nature may be, at least theoretically, solved. However, whenever both the magnitude and the direction of the velocity vary along a rigid boundary, then the Ω-plane is not in general composed of straight lines or of lines intersecting each other at suitable angles which would yield integrable transformations. Consequently, one will either seek other methods of handling the curved boundaries or completely abandon the direct approach of obtaining a solution for a given geometry. The indirect approach seeks a family of solutions for a set of jet-deflection and departure-angle conditions and then lets the designer choose the one best suited to his needs.

A relatively direct approach consists of rounding off of the corners of buckets otherwise composed of straight segments. Generally, this procedure results in a considerable complication of the mathematical problem and requires suitable analytical and physical simplifications. The existing methods may be classified as follows. Rounding off of the corners a) by assuming a constant pressure transition,[17] b) by assigning a special pressure distribution,[18] c) by modifying the t-plane and the corresponding terms in the Schwarz-Christoffel transformation[19] (a brief discussion of this method and the difficulties associated with it are also described by Carrier et al.),[20] and finally, d) through the use of special transformations such as Riemann-Hilbert transformation,[21,22] hodograph-plane transformations,[23] etc. As noted previously, some of these methods require the solution of complicated differential or integral-equation problems and some consist in first solving the problem with sharp corners and subsequently replacing the original boundary with a modified one having rounded corners. Often the time and effort required to round off the sharp corners may not be commensurate with the need for a solution and it may be desirable to adopt an indirect approach where the shape of the curved boundary is not initially known but obtained as part of the solution.

Levi-Civita's Method

Levi-Civita[15,24] may be said to have solved the inverse problem of describing the class of all two-dimensional jets divided by curved barriers. Although no specific solutions have been presented, the problems of determining such flows were reduced in special cases[25,26] to the solution of nonlinear integral equations with appropriate boundary conditions. The method has not previously been applied to the solution of the deflection of a two-dimensional jet from a finite two-dimensional curved boundary. It consists of the definition of a complex function ω as
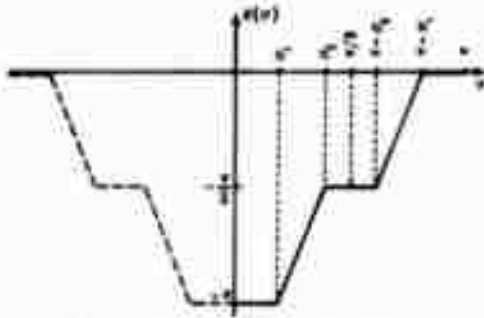
$$\omega = \theta + iLn(q/V_j) \qquad (1)$$

and the definition of the shape or the curvature of the obstacle in terms of the coefficients of a polynomial representing ω.

For the problem under consideration, the physical z-plane (see Fig. 1a) consists of a jet of width $2d$ and velocity V_j impinging upon a curved, symmetric, two-dimensional bucket BAB'. The complex-potential function W is given, as usual, by $W = \phi + i\psi$. A straightforward application of the Schwarz-Christoffel transformation establishes a relation between the t- and W-planes. Thus, one has

$$W = -(V_j d/\pi)[Ln(1-t) + Ln(1+t)] \qquad (2)$$

The parameter k in the t-plane is uniquely related to the deflection angle β.

Fig. 2 A typical representation of $\theta(\sigma)$.

The upper half of the t-plane is now transformed into the inner region of a semicircle of unit radius (see Fig. 1d) through the transformation given by Levi-Civita[24] as

$$t = -k(\zeta + \zeta^{-1})/2 \qquad (3)$$

The circular arc in Fig. 1d represents the solid boundary over which the direction of the velocity vector is assumed to be prescribed and the line BCDC'B' represents the free steamlines where the magnitude of the velocity is known.

The functions W and ω may be written as

$$-(1/V_j)(dW/dz) = (q/V_j)e^{-i\theta} \qquad (4)$$

and

$$\omega = iLn\left(-\frac{1}{V_j}\frac{dW}{dz}\right) = \theta + iLn(q/V_j) \qquad (5)$$

which, in terms of ζ, reduces to

$$\frac{z}{d} = -\frac{1}{V_j}\int e^{i\omega(\zeta)}\frac{dW}{d\zeta}d\zeta \qquad (6)$$

Defining $\zeta = r\exp(i\sigma)$ and noting that over the bucket only the argument and along the free streamlines only the modulus varies, the combination of Eqs. (2) and (6) yields,

$$\frac{z}{d} = \frac{1}{\pi}\int e^{i\omega(\sigma)}\frac{2k^2\cos\sigma\sin\sigma}{1-k^2\cos^2\sigma}d\sigma \qquad (7)$$

and

$$\frac{z}{d} = \frac{1}{\pi}\int e^{i\omega(\sigma)}\frac{k^2(r^2-r^{-2})/2r}{k^2(r+r^{-1})^2/4-1}dr \qquad (8)$$

where Eq. (7) gives the coordinates of the bucket and Eq. (8) the coordinates of the free streamlines.

The function ω is assumed, according to Levi-Civita, to be of the form

$$\omega(\zeta) = iLn[(i-\zeta)/(i+\zeta)] + a_o + a_1\zeta + a_2\zeta^2 + \ldots \qquad (9)$$

where the logarithmic term can be identified as that corresponding to a free jet impinging normally upon a flat plate.[25] The additional terms in the polynomial whose coefficients are to be prescribed later modify the expression for ω and give a suitable camber to the rigid boundary.

Noting that $a_2, a_4, a_6, \ldots$ must be taken equal to zero because of symmetry of the flow and that $r = 1$ over the solid boundary and $\sigma = 0$ or $\sigma = \pi$ over the free streamlines, Eq. (9) may be reduced over the bucket to

$$\omega(\sigma) = iLn\frac{|\cos\sigma|}{1+\sin\sigma} \pm \frac{\pi}{2} + a_1 e^{i\sigma} + a_3 e^{3i\sigma} + a_5 e^{5i\sigma} + \ldots \qquad (10)$$

where plus sign is to be used for $\pi > \sigma > \pi/2$, and minus sign for $\pi/2 > \sigma > 0$. Over the free streamlines, Eq. (9) reduces to

$$\omega(r) = -\tan^{-1}\frac{2r}{1-r^2} + a_1 r + a_3 r^3 + a_5 r^5 + \ldots \qquad (11)$$

The coefficients $a_1, a_3, \ldots$ may now be chosen to obtain different bucket shapes. In this study a Fourier-series representation was used primarily because of the versatility afforded by it in representing different bucket shapes. The evaluation of the coefficients requires a statement of the conditions at the tip and the axis of the bucket. Let the jet departure angle at the tip of the bucket be equal to $\pm\pi$, and the curvature at the stagnation point be continuous. Then one has

$$\omega(+1) = -\pi, \quad \omega(i) = \pm\pi/2 - i\infty, \quad \omega(-1) = \pi, \quad \omega(0) = 0$$

The relationship between $\theta(\sigma)$ and σ may be chosen at will. Let this relationship be represented by a simple, symmetric variation as shown in Fig. 2. Equation (10) may now be written as,

$$\omega(\sigma) = iLn\frac{\cos\sigma}{1+\sin\sigma} + ih(\sigma) + \theta(\sigma) \qquad (12)$$

where

$$h(\sigma) = \sum a_n \sin n\sigma, \qquad n = 1, 3, 5, \ldots \qquad (13)$$

and

$$\theta(\sigma) = -(\pi/2) + \sum a_n\cos n\sigma \qquad (14)$$

The coefficients a_n are given by

$$a_n = [2/(\sigma_1 - \sigma_2)n^2](\cos n\sigma_1 - \cos n\sigma_2) \qquad (15)$$

in which σ_1 and σ_2 represent the two parameters shown in Fig. 2. For $n = 0$, $a_o = -\pi/2$ as expected from the average value of the function $\theta(\sigma)$.

To complete the analysis one needs to evaluate the term $\exp[i\omega(\sigma)]$ which appears in Eqs. (7) and (8). Writing,

$$e^{i\omega(\sigma)} = [(1+\sin\sigma)/\cos\sigma]e^{-h(\sigma)}e^{i\theta(\sigma)} \qquad (16)$$

and separating the real and imaginary parts, one has

$$e^{i\omega(\sigma)} = (1+\sin\sigma)/\cos\sigma\, e^{-h(\sigma)}[\cos\theta(\sigma) + i\sin\theta(\sigma)] \qquad (17)$$

Combining Eqs. (7), (13), (15), and (17) one has

$$\frac{x}{d} = \frac{1}{\pi}\int_{\pi 2}^{\sigma} e^{-h(\sigma)}\frac{2k^2(\sin\sigma)(1+\sin\sigma)}{1-k^2\cos^2\sigma}\sin\theta(\sigma)d\sigma \qquad (18)$$

and

$$\frac{y}{d} = \frac{1}{\pi}\int_{\pi 2}^{\sigma} e^{-h(\sigma)}\frac{2k^2(\sin\sigma)(1+\sin\sigma)}{1-k^2\cos^2\sigma}\cos\theta(\sigma)d\sigma \qquad (19)$$
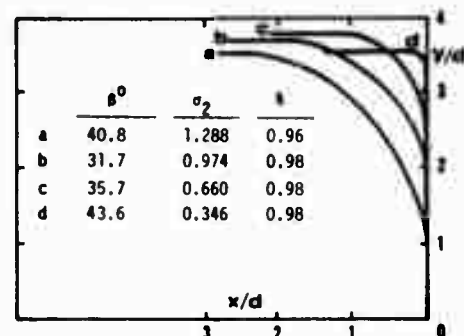
Equations (18) and (19) yield the coordinates of the curved boundary through the use of the appropriate values of σ_1 and σ_2. This in essence completes the application of the Levi-Civita's method to the analysis of the jet deflection from a two-dimensional curved bucket similar to that shown in Fig. 1.

The deflection angle is evaluated by replacing in Eq. (11) the corresponding value of r at the point C, i.e.,

$$r = [1 - (1-k^2)^{1/2}]/k \qquad (20)$$

The foregoing equations have been numerically integrated for a series of representative values of σ_1 and σ_2. The resulting family of bucket shapes are shown in Fig. 3. A special case for $\sigma_1 = 0.31416$ and $\sigma_2 = 0.47124$, and $k = 0.946$, ($\beta = 68°$), is shown in Fig. 4.

Evidently, Levi-Civita's method, with the novelties introduced into it in this study, is sufficient not only to generate a family of suitable two-dimensional curved reversers but also to round off the corners of buckets composed of straight segments. For example, by letting $(\sigma_1 - \sigma_2) \to 0$, one finds that the bucket shape generated by this method exactly approaches that previously solved by Sarpkaya.[2] For slightly larger values of $(\sigma_1 - \sigma_2)$, the corner PQ (see Fig. 4) is rounded off. This enables one, for example, to evaluate the sensitivity of the deflection angle to the rounding off of the sharp corner on a U-shaped bucket.

	$\beta°$	σ_2	k
a	40.8	1.288	0.96
b	31.7	0.974	0.98
c	35.7	0.660	0.98
d	43.6	0.346	0.98

x/d

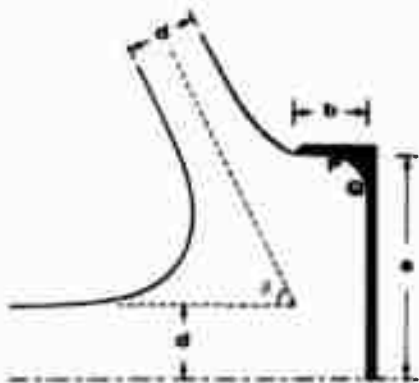Fig. 3 Family of two-dimensional curved buckets for $\sigma_1 = 0.31416$.

Fig. 4 A typical curved bucket for $\sigma_1 = 0.31416$, $\sigma_2 = 0.47124$, $k = 0.946$, $a/d = 3.05$, $b/d = 1.07$, and $\beta = 68°$.

The present work may be easily extended to the analysis of the cases where the lip angle of the bucket is other than π or the bucket has a cusp on its axis of symmetry or to the cases where the impinging jet is not entirely free and emerges from a prescribed nozzle.

Analysis of Axisymmetric Curved Deflectors

As noted earlier, the three-dimensional counterpart of the jet-deflection problem has not yet been solved in any generality. The finite-difference and relaxation techniques suffer in general from convergence and accuracy problems and nearly all resort to simple trial-and-error procedures to locate the free surfaces and to satisfy the boundary condition that the free surfaces be stream surfaces of constant velocity. In the following two fairly new methods, namely Belotserkovsky's[14] integral method and the finite element method are used to analyze representative axisymmetric cases.

Application of the Belotserkovsky's Method

Firstly, the coordinates s and n along and normal to the unknown axisymmetric free surface are chosen and the flow region is divided into three zones as shown in Fig. 5. Zone I represents the nozzle and the oncoming jet, Zone II represents the jet sheet formed over most of the bucket, and finally, Zone III represents the deflected jet. Zones I and II, and II and III are separated by the stagnation normal and the tip normal respectively.

Secondly, the functional forms of all the integrands appearing in the equations of motion are assumed and the equations are integrated to yield, through successive iterations, the relation-
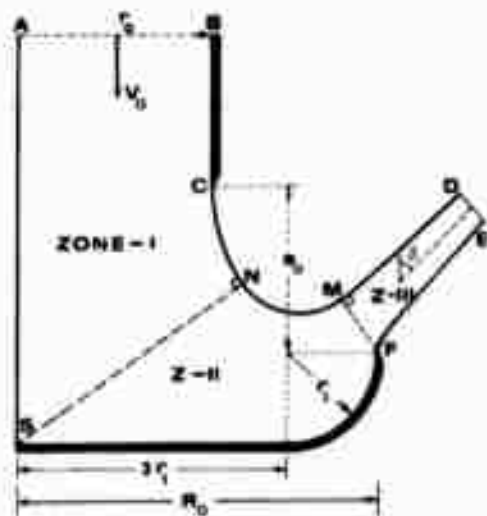

Fig. 5 A typical axisymmetric bucket and the definition of three zones of flow (SN: stagnation normal, MF: tip normal).
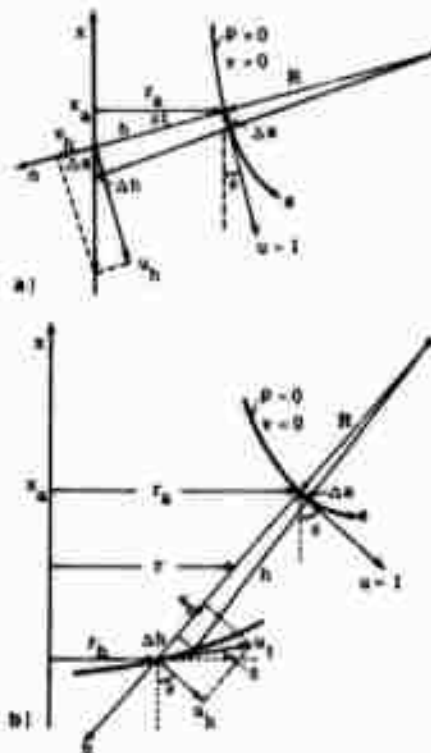

Fig. 6 Coordinate axes and geometrical relations a) in Zone I, b) in Zones II and III.

ships between the geometrical quantities describing the jet boundary and the values of the flow variables on the boundaries.

Dividing all velocities by the freestream velocity V_j, all pressures by $0.5\rho V_j^2$, and all lengths by the nozzle radius r_o, one writes in s-n coordinates (see Fig. 6a) with corresponding velocity components u and v the continuity and momentum equations for a steady, incompressible, axisymmetric, inviscid flow as,[13]

$$\frac{d}{ds}\int_o^h (ru)\,dn - (ru)_h \frac{dh}{ds} + \left(1 + \frac{h}{R}\right)(rv)_h = 0 \qquad (21)$$

and

$$2\frac{d}{ds}\int_o^h (ruv)\,dn - 2(ruv)_h \frac{dh}{ds} + \left[\left(1 + \frac{n}{R}\right)r(2v^2 + p)\right]_h -$$
$$\int_o^h \frac{r}{R}(2v^2 + p)\,dn + \cos\theta \int_o^h \left(1 + \frac{n}{R}\right)p\,dn = 0 \qquad (22)$$

where index h means evaluation of the quantity within the parentheses or brackets at $n = h$ and R represents the radius of curvature in the meridional plane of the free jet surface. In the derivation of the above equations implicit is the condition that $p = v = 0$ at $n = 0$.

A first approximation to the problem is usually obtained by assuming the velocities vary linearly with n, i.e.,

$$u = 1 - (n/h)(1 - u_h), \qquad v = (n/h)v_h \qquad (23)$$

where u_h and v_h are the unknown values of u and v along the axis of symmetry in Zone I and along the rigid boundary in Zone II (see Fig. 6b). Then Eq. (21) at the nozzle exit reduces to

$$u_h = 3V_o - 2 \qquad (24)$$

For nozzles for which there is no back-pressuring effect due to the bucket proximity; i.e., for large values of s_o (see Fig. 5), one has $V_o = u_h = 1$.

In Zone I, Eq. (21) reduces to

$$r_a h(2 + u_h) = 3 \qquad (25)$$

and Eq. (22) takes the form

$$2\frac{d}{ds}\int_o^h (ruv)\,dn - \frac{1}{R}\int_o^h r(2u^2 + p)\,dn + \cos\theta\int_o^h \left(1 + \frac{n}{R}\right)p\,dn = 0 \qquad (26)$$

which reduces through the use of the geometrical relationships and Eqs. (23) and (25) to

$$A \frac{d\theta}{ds} + B = 0 \tag{27}$$

in which A and B are functions of h, u_t, and θ and were previously given by Ryhming [13]

In Zone II, Eqs. (21) and (22) reduce to

$$h(2r_a + r_h) + u_h h(r_a + 2r_h) = 3 \tag{28}$$

and

$$P \frac{d\theta}{ds} + Q = 0 \tag{29}$$

in which P and Q are functions of h, u_h, r_h, δ, and θ.[13]

In Zone III, the equations derived for Zone II hold true except that $p = 0$, everywhere, since $u_t = 1$ and

$$u_h = \sin(\theta - \delta) \tag{30}$$

$$v_h = \cos(\theta - \delta) \tag{31}$$

Zones I, II, and III are related by the conditions pertaining to the stagnation normal SN and the tip normal FM (see Fig 5). Noting that at the stagnation point S, $x = 0$, $r_h = 0$, and $u_h = 0$, one has from Eq. (28), for the stagnation normal, the condition

$$h^2 \cos \theta = 1.5 \tag{32}$$

Similarly, noting that for the case under consideration $\delta = \pi/2$, (the tangent to the lip of the bucket is taken parallel to the x-axis), one has, for the tip normal, the condition

$$h^2(2 \cos \theta - \cos^2 \theta) - 3hr_h(\cos \theta - 1) = 3 \tag{33}$$

Equation (32) defines a curve $h = h(\theta)$ on which the end points of all possible stagnation normals have to lie, which pass through the stagnation point S. Equation (33) defines a similar curve on which all possible tip normals lie.

The foregoing equations were used to analyze the deflection of axisymmetric jets from buckets composed of a flat plate and a quarter circle as shown in Fig. 5. The calculations were performed as follows. First, a deflection angle β and the nozzle velocity V_o were assumed. Then the thickness of the jet $DE = d$, and the coordinates r_t and r_D were calculated from the equation of continuity. Obviously, d, r_t, and r_D are subsequently recalculated on the basis of the iterated value of V_o. The point E is connected to the point F (the lip of the bucket) by a straightline as a first approximation to the upper free surface and the line EF is temporarily regarded as a rigid boundary.

The governing equations were programmed according to a standard Runge-Kutta sub-routine and then iterated as follows. The calculations started at the tip of the nozzle where $\theta = 0$ and $u_h = 3V_o - 2$ and proceeded along the free surface. The coordinates of the free streamline, h, and θ were calculated at suitable intervals. Finally, a point was reached at which Eq. (32), (the stagnation normal condition) was satisfied. Clearly, the stagnation normal can intersect the x-axis at a point other than $x = 0$ and still satisfy Eq. (32). Thus, it was necessary that $x = 0$ at $r_h = 0$, i.e., the stagnation point must be located on the bucket. To this end, the velocity V_o was iterated upon until both conditions [Eq. (32) and $x = 0$ at $r_h = 0$] were satisfied. Physically, this iteration corresponds to the first order calculation of the back-pressuring effect of the bucket proximity on the nozzle flow.

Integration of the Eq. (29) in Zone II begins at first with the x_a, r_a, h, θ, and R values calculated at the end of the Zone I. The free streamline calculated with these initial values define a spline shift (see Fig. 7) due to the saddle-point character of the equations at the singular point. Consequently, a sequence of points along the initial curve defined by Eq. (32) are chosen, and the corresponding integral curves are calculated. These, in turn, determine an upper and a lower bound for the proper location of the desired solution. The process is then repeated until a sufficiently accurate bound is determined. The above procedure requires about ten iterations. The consequence of the saddle-point character of the equations in the vicinity of the

stagnation normal is that there is a sector of overlap in the jet, going upstream and downstream from the stagnation normal. A similar behavior has been found previously with the Belotserkovsky method in similar situations using a first-order scheme.[13,27] Integration in Zone II is terminated at the tip normal at which Eq. (33) is satisfied.

The determination of the shape and position of the deflected jet in Zone III requires three kinds of successive iterations. The first is the determination of the appropriate values of h and θ at the tip normal which satisfy Eq. (33) and yield a sufficiently long portion of the integral curve between the upper and lower bounds. This iteration yields a lower free surface with zero pressure and unit freestream velocity but the freestream conditions ($u_t = 1$, $p = 0$) at the upper surface are not yet satisfied since the upper surface was initially assumed to be a solid boundary. Furthermore, the calculated stream surface does not necessarily coincide with the assumed lower free surface because the assumed jet-deflection angle is either larger or smaller than the actual deflection angle. This, in turn, requires an iteration on β. For this purpose, the point D is located on the calculated lower free surface and the new values of r_t, r_D, and d are calculated from the equation of continuity. The rotation of the upper free surface constitutes a first-order correction to the deflection angle β. Then the calculations noted above were repeated until the deflection angle did not change more than $2°$. This required from five to ten iterations depending on the initially assumed value of the jet-deflection angle.

The third kind of iteration was made to determine the position and curvature of the upper free surface. As noted earlier FE was initially assumed to be a straight rigid boundary and thus the calculated tangential velocities along it were not everywhere equal to unity, particularly in the vicinity of the lip of the bucket. Then the points on the upper boundary were moved inward, along the n-axis if $u_t > 1$ and vice verse by an amount

$$\Delta n = \lambda(u_t^2 - 1) \tag{34}$$

in which λ is an assigned multiplier and u_t is the previously calculated tangential velocity. Experience has shown that the iteration will converge even for a very crudely assumed boundary for a value of $\lambda = 0.10$. As to the reason for using $(u_t^2 - 1)$, it was simply for the purpose of accentuating the error and accelerating the correction of the boundary points at which the velocities most differ from unity. At the end of each iteration, the corrected boundary was smoothened through the use of a generally available CURVEFIT subroutine by passing a smooth curve through the calculated points and recalculating the intermediate points. Then all three types of iterations on the lower and upper boundary were repeated until the velocities everywhere were within 1 ± 0.05. The results of a typical case calculated in the manner described above is shown in Fig. 5 in which $\beta = 44.5$.
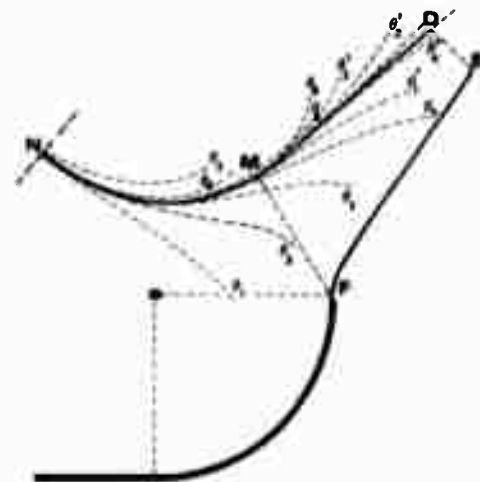

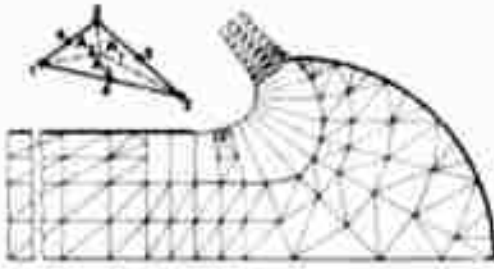Fig. 7   Spline shift in Zones II and III.

Fig. 8   Finite element representation of jet deflection from a hemispherical reverser.

It is evident from the foregoing that the Belotserkovsky's integral method has certain limitations. Firstly, the assumption of a linear velocity along s and n coordinates cannot be valid for all bucket shapes and relative jet radii. The variation of u near the free surface is rather large particularly for very deep buckets. In such cases Belotserkovsky's method may produce rather complex and physically unacceptable flow situations in the vicinity of the stagnation point. Although no specific criteria can be developed for the bucket shapes to which the Belotserkovsky's method can be successfully applied, it may be recommended on the basis of the present study that the bucket radius be larger than $1.5r_o$ and the bucket depth be smaller than $2r_o$. Clearly, the specification of the radius of curvature alone at the stagnation point in terms of the jet radius is not sufficient. As to the merits of the method, it is rather straightforward and yields, within the ranges of the parameters recommended, results which are sufficiently accurate for the calculation of the pressure distribution on the bucket and the reverser thrust.

Application of the Finite Element Method

Zienkiewicz and Cheung[28] proposed in 1965 the application of the finite element method to the solution of field problems involving the equations of Laplace and Poisson. Since then a significant number of applications of the finite element method to fluid dynamics has appeared in the literature.[29] The method has recently been applied to several jet-efflux problems involving only one freestream surface and relatively small jet contraction by Chan[30] and Chan and Larock.[31]

The present analysis is devoted to a determination of the angle of deflection, the location of the freestream surfaces, and the velocity and pressure distributions caused by a finite curved bucket placed symmetrically with respect to the axis of an axisymmetric, inviscid jet issuing from a uniform nozzle.

The governing equation is then given by

$$\phi_{,xx} + \phi_{,r}/r + \phi_{,rr} = 0 \tag{35}$$

For an axisymmetric flow, the solution to the Laplace-field equation satisfying the specified normal-velocity conditions $(\phi_{,n})^a$ is given by that admissible function ϕ which minimizes the functional[32]

$$I(\phi) = \pi\rho \iint_A \left[(\phi_{,x})^2 + (\phi_{,r})^2\right] r\, dr\, dx - 2\pi\rho \int_C \phi(\phi_{,n})^a r\, ds \tag{36}$$

in which A is the half of a meridional section of the flow and C is a portion of the curve bounding this area where the normal derivative is prescribed. The first integral in Eq. (36) represents the kinetic energy of the fluid within the entire control volume and the second integral represents twice the work done by the impulsive pressure $\rho\phi$ on the boundaries in starting the motion from rest.

The approximate minimization of the functional $I(\phi)$ is accomplished by dividing the field of interest into N triangular elements, with corner and midpoint nodes, and writing

$$I(\phi) = \sum_1^N I^e(\phi) \tag{37}$$

The variation of ϕ within each element is represented by a second-order polynomial. The use of higher order polynomials leads to extremely tedious arithmetical manipulations. In terms of the area coordinates $\zeta_i = A_i/A^m$ (see Fig. 8); this leads to

$$\phi^m = \zeta_1(2\zeta_1 - 1)\phi_1 + \zeta_2(2\zeta_2 - 1)\phi_2 + \zeta_3(2\zeta_3 - 1)\phi_3 + $$
$$4\zeta_1\zeta_2\phi_4 + 4\zeta_2\zeta_3\phi_5 + 4\zeta_1\zeta_3\phi_6 \tag{38}$$

The velocity components are given by

$$v_x{}^m = \phi_{,x}{}^m \quad \text{and} \quad v_r{}^m = \phi_{,r}{}^m \tag{39}$$

The substitution of Eqs. (38) and (39) in Eq. (36) and the use of the Ritz technique yield,

$$\partial I^m(\phi)/\partial \phi_i = SA_{ij}{}^m \phi_j{}^m - SLA_i{}^m = 0 \tag{40}$$

in which $SA_{ij}{}^m$ and $SLA_i{}^m$ represent respectively the element-stiffness matrix and the corresponding load matrix for a triangular element. Chan and Larock[31] who tabulated $SA_{ij}{}^m$ and $SLA_i{}^m$, assumed, in the derivation of the matrix $SLA_i{}^m$, a constant normal velocity on a boundary side of an element. This condition which conflicts with the linear interpolation of the velocity field has been relaxed along the lines recommended by Kotchergenko and Amorim[33] and the coefficients $SLA_i{}^m$ have been corrected accordingly.

Iteration Scheme

As cited earlier, the deflected jet is characterized by two initially unknown axisymmetric freestream surfaces. Thus special attention must be focused on finding a suitable iterative procedure for systematically approaching the final positions of the boundaries. The iteration is terminated when the boundary conditions are satisfied within a prescribed absolute maximum error. The boundary condition to be satisfied is that the free surfaces be streamlines of constant velocity.

The grid is divided into two major regions. The first region consists of elements whose coordinates are fixed once for all (see Figs. 8 and 9). This region is well within the interior of the flow and is not expected to be intersected by the freestream surfaces. The second region, i.e. the moving grid, consists of elements whose coordinates are recalculated each time the free surface is moved. The movement of the grid is made in such a manner that each element maintains a shape more or less compatible to its original shape. The grid inside the exiting jet (along FE in Fig. 9) is relocated by moving each middle node to its correct position between two opposite nodes on each side of the jet, (see Fig. 8). In regions of high velocity, relatively small triangles and in regions of rather low velocity, larger triangles are used. The example shown in Fig. 8 contains 288 elements and 683 nodal points. The bandwidth was 60.

Iteration of the free surfaces began with the assumption of a deflection angle β and the sketching of the two free surfaces as carefully as possible on the basis of past experience. Then the assumed boundaries were regarded as rigid boundaries. The nozzle length was varied from $2r_o$ to $6r_o$ and the jet length FE from $0.6r_o$ to r_o in various programs with no noticeable difference in the results. The thickness of the jet $DE = d$, and the radial coordinates r_E and r_D (see Fig. 9) were calculated from the equation of continuity by assuming $V_o = 1$. Obviously, d, r_E, and r_D are subsequently recalculated on the basis of the iterated
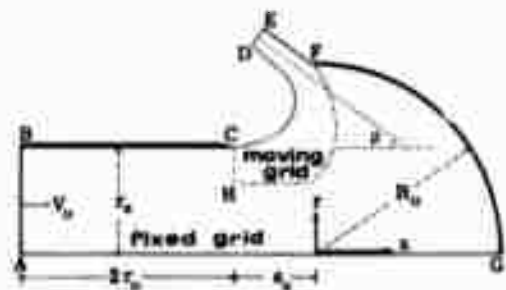

Fig. 9   Half meridian plane of jet flow and the two grid system.

Table 1 The comparison of numerical and experimental results for axisymmetric thrust reversers

Reverser type	R_o/r_o	s_o/r_o	β (deg) (theory)	β (exper) (present)	η_R (theory)	η_R (exper)[a] (Ref. 34)	η_R (exper)[b] (present)	Nozzle pressure ratio
Fig 9	1.90	0.10	18.5	10	0.76	0.81	0.78	2
Fig 9	1.80	0.40	20.3	13	0.77	0.82	0.80	2
Fig 9	1.70	0.60	46.8	39	0.65	0.81	0.74	2
Fig. 9	1.60	0.80	50.5	47	0.52	0.74	0.60	2
Fig 9	1.50	0.90	61.1	57	0.39	0.61	0.44	1.8
Fig 9	1.80	0.80	35.2	31	0.73		0.75	1.8
Fig 5[c]	1.80	0.80	44.5	40	0.69		0.73	2
Fig 5[d]	1.80	0.80	43.2	40	0.71		0.73	2

[a] With a boattail
[b] With a sharp-edged straight nozzle
[c] Through the use of Belotserkovsky's method
[d] Through the use of the finite element method

values of V_o. The point E is connected to the point F by a straight line as a first approximation to the upper free surface.

The first run through the computer calculates the velocity at C (see Fig. 9), i.e., at the lip of the nozzle. It turns out to be larger than unity (the correct value is $V_C = 1$) since V_o is assumed to be equal to unity. V_o is immediately corrected, to a first-order of approximation, by writing

$$V_o^k = V_o^{(k-1)} - (V_C^{(k-1)} - 1)V_o^{(k-1)} \qquad (41)$$

which is used in all subsequent iterations. Then r_L, r_D, and d are recalculated as in the case of the application of the Belotserkovsky's method.

The procedure which has enabled the assumed boundaries to converge in a systematic manner to their final positions may be described as follows. Let the velocity at an arbitrary point along the assumed boundary be V_s. Then the boundary is moved inward, along a line normal or nearly normal to the boundary, if $V_s > 1$ and vice versa by an amount

$$\Delta n = \lambda(V_s^2 - 1) \qquad (42)$$

In these calculations, the multiplier λ was taken equal to 0.015. At the end of a given number of iterations, the velocities along one or both boundaries may approach values other than unity because the assumed deflection angle is not necessarily the correct one. Clearly, the deflection angle adjusts itself at the end of each iteration but this adjustment is rather small (about 0.2°). Thus, for a large correction in β, say 20°, about 100 iterations are needed. Instead, five iterations were carried out for the assumed deflection angle and then β was incremented by 2°, clockwise or counter-clockwise depending on whether the velocities in the upper free surface was smaller or larger than unity. When the velocities everywhere were within 1 ± 0.05, β was no longer incremented by 2° and the number of iterations was increased to 25. The calculations were terminated when the velocities everywhere were within 1 ± 0.015. The entire iteration for a given nozzle-reverser geometry required approximately 30 mins on an IBM-360/67 computer. The program was written in FORTRAN and double-precision arithmetic was used.

Examples and Results

The method and the procedures described above have been used to analyze the characteristics of axisymmetric-jet deflection from hemispherical (see Fig. 8) as well as fairly shallow (see Fig. 5) target-type thrust reversers. This type of reversers give the desired amount of reverse thrust without affecting the engine operation and lend themselves to stowage with a minimum amount of boattail or base drag.

The geometry of the nozzle-reverser combination is uniquely defined by the ratios R_o/r_o and s_o/r_o (see Figs. 5 and 9) once the bucket and nozzle shape are decided upon. It is clear, at least from the experiments[34] that there is a unique combination of R_o/r_o and s_o/r_o for which the reverse thrust is maximum. The determination of this combination and the calculation of the resulting thrust constitute the essence of the practical problem.

In the aircraft industry, the efficiency of a thrust reverser is expressed in terms of a "reverse-thrust ratio" η_R defined by the ratio of the actual reversed-jet thrust to the forward jet thrust of the nozzle alone. In other words, η_R is given by

$$\eta_R = (\pi \rho r_o^2 V_o V_j \cos \beta)/(\pi \rho r_o^2 V_j^2) = (V_o/V_j) \cos \beta \qquad (43)$$

Evidently, $\eta_R = \eta_R(R_o/r_o, s_o/r_o)$ since both V_o and β depend on R_o/r_o and s_o/r_o for a family of geometrically similar reversers. In passing it should be noted that the error made in the calculation of η_R by assuming the jet leave the deflector exactly parallel to the tangent at the lip of the deflector, i.e., by writing $\beta = 0$, as was done by Schnurr et al., would be (assuming V_o remains relatively unaffected) nearly proportional to $(1 - \cos \beta)$. This error could be rather large particularly for large angles of deflection and its correction through the use of another arbitrary parameter such as the "spillage coefficient" introduced by Schnurr et al.[12] is not justified. Evidently, the correct calculation of thrust requires the determination of the deflection angle.

The results of the finite element analysis and their comparison with those obtained experimentally are presented in Table 1 together with those obtained through the use of the Belotserkovsky's method. The experimental values of η_R are somewhat larger than those obtained numerically. There are several reasons for this difference; the two most important ones being the Coanda effect (see, e.g., Ref. 35) and the nozzle pressure ratio. The Coanda effect, i.e., the tendency of a jet to attach to adjacent surfaces (in this case to the outer surface of the nozzle) because of the entrainment deprivation, decreases the deflection angle and thereby increases the reversed thrust. In the experiments conducted by Steffen et al.,[34] the outer surface of the nozzle was streamlined in the form of a boattail to decrease entrainment and thus to increase η_R. In fact, as noted by Steffen et al., "the pressure reductions on the boattail were large enough to account for as much as 20% of the reverse-thrust ratio." Thus the relatively large differences between the η_R values experimentally obtained by Steffen et al. and those predicted numerically are primarily attributable to the Coanda effect.

The present experiments were conducted with a straight, sharp-edged nozzle ($r_o = 1.32$ to 1.57 in., $R_o = 2.5$ in.) and the effect of the jet attachment has been minimized. This has resulted in a closer agreement between the computed and experimental values of η_R. In passing it should be noted that the Coanda effect is not necessarily desirable, in spite of its contribution to the reverse thrust, for it may cause an unstable flowfield and destructive vibrations.

The nozzle-pressure ratio or the actual velocity in the nozzle causes variations in η_R primarily because the entrainment needs of the deflected jet and hence the Coanda effect increase with increasing jet velocity. Consequently, η_R increases (about 10 percentage points) over a range of nozzle-pressure ratios from 1.7 to 3.

Table 1 shows that the relative spacing of the nozzle and the reverser size significantly affect the flow reversal. Evidently, η_R

increases with an increase in hemisphere diameter and reaches a maximum of about 80% for $R_o/r_o = 1.8$ and $s_o/r_o = 0.40$. This nearly corresponds to an optimum nozzle-reverser spacing. Extensive experimental data obtained by Steffen et al.[34,36] with various types of reversers clearly show that at spacings greater than that required for optimum performance, η_R may drop as much as 20%. Closer spacings do not noticeably affect the reverser performance but result in decreased flow rate for a given total nozzle pressure or in increased pressure for a given flow rate because of the increased blockage or back-pressuring effect of the reverser.

Conclusions

Though the equations for jets impinging on curved surfaces are not integrable in a closed form, the behavior of their solutions is predictable through the use of numerical methods. For two-dimensional cases, the Levi-Civita method provides a variety of bucket shapes and enables one to round off the sharp corners of buckets otherwise composed of straight segments. For these cases, the finite element method could also provide direct solutions for prescribed boundary shapes.

The Belotserkovsky and finite element methods may be used with confidence for the analysis of an axisymmetric Laplace field where one or more parts of the boundary are to be determined as part of the solution. In particular, these methods are capable of predicting the idealized-performance characteristics of axisymmetric thrust reversers. Evidently, some of the practical problems associated with thrust reversal, such as the reattachment of the jet to the nacelle of the engine, hot-gas reingestion, interaction of the deflected jet with the ambient stream, noise intensification, etc., require additional analytical and experimental investigation.

References

[1] Taylor, G. I., "Oblique Impact of a Jet on a Plane Surface," *Philosophical Transactions of the Royal Society of London*, Vol. 260A, 1966, pp. 96-100.

[2] Sarpkaya, T., "Deflection of Jets, II-Symmetrically Placed U-Shaped Obstacle," *Studies in Engineering*, No. 35, 1953, pp. 45-53, State Univ. of Iowa, Iowa City, Iowa.

[3] Tinney, E. R., Barnes, W. E., Richard, O. W., and Ingram, G. R., "Free-Streamline Theory for Segmental Jet Deflectors," *Journal of the Hydraulics Division*, American Society of Chemical Engineers, Vol. 87, No. HY5, Sept. 1961, pp. 135-145.

[4] Chang, H. Y. and Conly, J. F., "Potential Flow of Segmental Jet Deflectors," *Journal of Fluid Mechanics*, Vol. 46, Pt. 3, April 1971, pp. 465-475.

[5] Schach, W. V., "Umlenkung eines freien Flussigkeitsstrahles an einer ebenen Platte," *Ingenieur Archive*, Vol. 5, 1934, pp. 245-265.

[6] Trefftz, E., "Uber die Kontraktion Kreisformiger Flussigkeits-Strahlen," *Zeitschrift fuer Angewandte Mathematik und Physik*, Vol. 64, May 1917, pp. 34-42.

[7] Jeppson, R. W., "Inverse Formulation and Finite Difference Solution for Flow from a Circular Orifice," *Journal of Fluid Mechanics*, Vol. 40, Pt. 1, Jan. 1970, pp. 215-223.

[8] Southwell, R. and Vaisey, G., "Relaxation Methods Applied to Engineering Problems," *Philosophical Transactions of the Royal Society of London*, Vol. 240A, 1948, pp. 117-161.

[9] Rouse, H. and Abul-Fetouh, A., "Characteristics of Irrotational Flow through Axially Symmetric Orifices," *Journal of Applied Mechanics*, Vol. 17, June 1950, pp. 421-426.

[10] Garabedian, P., "Calculation of Axially Symmetric Cavities and Jets," *Pacific Journal of Math.*, Vol. 6, 1956, pp. 611-684.

[11] Hunt, B. W., "Numerical Solution of an Integral Equation for

Flow from a Circular Orifice," *Journal of Fluid Mechanics*, Vol. 31, Pt. 2, Jan. 1968, pp. 361-377.

[12] Schnurr, N. M., Williamson, J. W., and Tatom, J. W., "An Analytical Investigation of the Impingement of Jets on Curved Deflectors," *AIAA Journal*, Vol. 10, No. 11, Nov 1972, pp. 1430-1435.

[13] Ryhming, I. L., "An Approximate Solution of the Steady Jet Impact Problem," *Journal of Applied Mathematics and Physics(ZAMP)*, Vol. 25, Oct. 1974, pp. 515-531.

[14] Belotserkovsky, O. M., "Flow Past a Circular Cylinder with a Detached Shock Wave," *Doklady Acad. Nauk SSSR*, Vol. 113, 1957, pp. 509-516.

[15] Birkhoff, G. and Zarantonello, E. H., "Curved Obstacles," *Jets, Wakes, and Cavities*, Academic Press, New York, 1957, pp. 130-135.

[16] Milne-Thomson, L. M., "Helmholtz Motions," *Theoretical Hydrodynamics*, Macmillan, London, 1968, pp. 336-339.

[17] Gerber, R. and McNown, J. S., "Transition Curves of Constant Pressure, I. Streamlined Struts," *Studies in Engineering*, No. 35, State Univ. of Iowa, Iowa City, Iowa, 1953, pp. 15-32.

[18] Schieldrop, E. B., "Two-Dimensional Fluid Motion Bounded by Straight and Curved Fixed Walls and Free Surfaces," *Skrifter Utgitt av Det Norske Videnskaps-Akademi I*, Oslo, Norway, Vol. 3, No. 6, 1928, pp. 437-444.

[19] Cockroft, J. D., "The Effect of Curved Boundaries on the Distribution of Electrical Stress Round Conductors," *Journal of the Institution of Electrical Engineers*, Vol. 66, June, 1928, pp. 385-409.

[20] Carrier, G. F., Krook, M., and Pearson, C. E., "Conformal Mapping," *Functions of a Complex Variable*, McGraw-Hill, New York, 1966, pp 154-156.

[21] Larock, B. E. and Street, R. L., "A Riemann-Hilbert Problem for Nonlinear, Fully Cultivating Flow," *Journal of Ship. Research*, Vol. 9, July 1965, pp. 170-177.

[22] Larock, B. E., "Jets from Two-Dimensional Symmetric Nozzles of Arbitrary Shape," *Journal of Fluid Mechanics*, Vol. 37, Pt. 3, July 1969, pp. 479-489.

[23] Sarpkaya, T. and Hiriart, G., "Potential Flow of Curved Jet Deflectors," *Proceedings of the 4th CANCAM*, Vol. 1, 1973, pp. 665-666.

[24] Levi-Civita, T., "Scie e Leggi di Resistenza," *Rendi Circulara Matematica*, Vol. 23, 1907, pp. 1-37.

[25] Cisotti, V., "Vene Fluenti," *Circulara Matematica*, No. 2, Palermo, Vol. 25, 1908, pp. 145-179.

[26] Wu, T. Y., "A Free Streamline Theory for Two-Dimensional Fully Cavitated Hydrofoils," *Journal of Mathematics and Physics*, Vol. 35, Pt. 3, 1956, pp. 236-265.

[27] Traugott, S. C., "An Approximate Solution of the Direct Supersonic Blunt-Body Problem for Arbitrary Axisymmetric Shapes," *Journal of Aero Space Science*, Vol. 27, 1960, pp. 361-372.

[28] Zienkiewicz, O. C. and Cheung, Y. K., "Finite Elements in the Solution of Field Problems," *The Engineer*, London, Vol. 24, 1965, pp 507-510.

[29] Oden, J., Zienkiewicz, O. C., Gallaher, R. H., and Taylor, C., eds., *Finite Element Methods in Flow Problems*, UAH Press, Huntsville, Ala., 1974.

[30] Chan, S. T. K., "Finite Element Analysis of Irrotational Flows of an Ideal Fluid," Ph.D. thesis, Dept. of Civil Engineering, 1971, Univ. of California at Davis, Davis, Calif.

[31] Chan, S. T. K and Larock, B. E., "Fluid Flows from Axisymmetric Orifices and Valves," *Journal of Hydraulics Division*, ASCE, Vol. 99, No. HY1, 1973, pp. 81-95.

[32] Norrie, D. A. and de Vries, G., "The Laplace or Potential Field," *The Finite Element Method — Fundamentals and Applications*, Academic Press, New York, 1973, pp. 193-196.

[33] Kotchergenko, I. D. and de Amorim, A. M. A., Discussion of Ref. 31, *Journal of Hydraulics Division*, ASCE, Vol. 100, No. HY3, 1974, pp. 497-498.

[34] Steffen, F. W., McArdle, J. G., and Coats, J. W., "Performance Characteristics of Hemispherical Target-Type Thrust Reversers," RM E55E18, June, 1955, NACA

[35] Sarpkaya, T., "Of Fluid Mechanics and Fluidics and of Analysis and Physical Insight," *Proceedings of the 5th Cranfield Fluidics Conference*, BHRA, Vol. 5, 1972, pp. 33-54

[36] Steffen, F. W., Krull, H. G., and Ciepluch, C. C., "Preliminary Investigation of Several Target-Type Thrust Reversal Devices," RM E53L15b, March, 1954, NACA